that GPIbα polymorphisms are clinically significant. Molecular mechanisms for the association between thrombus formation and those polymorphisms, however, are not yet clearly understood. To elucidate the effects of $^{145}$Thr/Met and/or VNTR polymorphisms on interactions with VWF, we performed two series of experiments; (a) ristocetin-induced $^{125}$I-labelled VWF binding to two recombinant fragments containing a partial GPIbα sequence ($^{1}$His–$^{302}$Ala) with either $^{145}$Thr (145T) or $^{145}$Met (145M), and (b) the interaction between immobilized VWF and four types of Chinese hamster ovary (CHO) cells expressing full-length GPIbα/β/IX, $^{145}$Thr/1R (T1R), $^{145}$Met/1R (M1R), $^{145}$Thr/4R (T4R), or $^{145}$Met/4R (M4R), under flow conditions.

## Methods

### *Preparation of recombinant GPIbα fragments*

The GPIbα insert of a pBluescript KS (−) construct, which contained a cDNA encoding a partial GPIbα sequence ($^{1}$His–$^{302}$Ala) with $^{145}$Thr, was cloned (Murata *et al*, 1991). The $^{145}$Thr/Met substitutions on the GPIbα insert were performed using Quick Change™ (Stratagene, La Jolla, CA, USA), and each insert was ligated with a expression vector pcDNA3·1Zeo (−) (Invitrogen, Groningen, The Netherlands). Each construct was sequenced to ensure that the introduced mutation was restricted to residue 145 and then transfected into CHO cells (Dainippon Pharmaceutical Co., Osaka, Japan) using FuGENE™ 6 Transfection Reagent (Roche, Nutley, NJ, USA). Cells were cultured in the presence of 300 μg/ml of zeocine (Invitrogen) for selection of stable transfectants. Culture medium containing secreted soluble protein was collected from 145T-, 145M-, or mock-transfected cells after serum-free culture medium for 48 h.

### *Quantitation and immunologic evaluation of recombinant proteins*

The expression of each recombinant protein was confirmed by Western blot analysis with anti-GPIbα monoclonal antibody, LJ-Ibα1 (a generous gift from Dr Z.M. Ruggeri, The Scripps Research Institute, La Jolla, CA, USA), which recognizes an epitope within the 45-kDa domain and reacts strongly with the reduced GPIbα fragment, using an enhanced chemiluminescence (ECL) Western blotting system™ (Amersham Pharmacia Biotech, Buckinghamshire, UK). The amounts were measured by dot-blot analysis with LJ-Ibα1 and $^{125}$I-anti-mouse IgG (Daiichi Pure Chemicals, Tokyo, Japan). Purified recombinant GPIbα (Moriki *et al*, 1997) was used as a standard. Equivalent amounts of 145T and 145M were evaluated for their immunologic reactivity toward a panel of anti-GPIbα monoclonal antibodies, LJ-P3 (a generous gift of Dr Z.M. Ruggeri, The Scripps Research Institute), GUR83–35 (Takara Shuzo, Shiga, Japan), and GUR20–5 (Takara Shuzo), which recognize conformation-specific epitopes within the 45-kDa domain (Handa *et al*, 1986; Vicente *et al*, 1988; Kawasaki *et al*, 1995; Ikeda *et al*, 2000). $^{125}$I-anti-mouse IgG was used as a secondary antibody in this quantitative analysis. A constant concentration (2 ng/μl) of 145T and 145M was used for subsequent functional analysis.

### *Ristocetin-induced $^{125}$I-VWF binding to immobilized recombinant GPIbα fragment*

Human VWF was provided by WelFide Co. (Osaka, Japan), and was radiolabelled with $^{125}$I (Amersham Pharmacia Biotech) according to the IODO-GEN procedure (Fraker & Speck, 1978). The analysis of ristocetin (final concentration, 1·0 mg/ml)-induced $^{125}$I-labelled soluble VWF (final concentration, 1·0 ug/ml) binding to immobilized 145T or 145M (400 ng/spot) was performed using the enzyme-linked immunofiltration assay apparatus (Pierce Chemical Co., Rockford, IL, USA). Details of this assay were described previously (Murata *et al*, 1991; Moriki *et al*, 1997). In the Scatchard plot analysis for the binding of $^{125}$I-VWF (0·5–16 ug/ml) to 145T or 145M, the dissociation constant was analysed by a simple regression model. It was assumed that the same proportion of VWF multimers binds to each recombinant protein, and that the molecular weight of VWF was 220-kDa.

### *Establishment of CHO cells expressing the GPIbαβIX complex*

A stable transfectant for GPIbβIX-expressing CHO cells was established, as described previously (Suzuki *et al*, 1999). A cDNA encoding the GPIbα sequence was cloned into a pBluescript KS (−) as described previously (Suzuki *et al*, 1999) and was subcloned into a mammalian expression vector pcDNA 3·1 Hygro (+) (Invitrogen) using the restriction sites for Kpn I (Takara Shuzo) and Not I. We prepared four types of plasmids for expression, T1R, M1R, T4R, and M4R. $^{145}$Thr/Met substitution was created by polymerase chain reaction (PCR)-based site-directed mutagenesis using Quick Change™ (Stratagene), and then inserted into the 1R or 4R sequences; PCR was performed on genomic DNA with the 1R and 4R alleles, followed by subcloning using a TA cloning kit (Invitrogen). Each insert was subsequently cloned into the GPIbα-pcDNA 3·1 Hygro (+) using Xba I restriction sites and sequenced. Each plasmid was transfected into GPIbβIX-expressing CHO cells using FuGENE™ 6. These cells were grown in culture medium with 800 μg/ml of G418, 300 μg/ml of zeocine, and 400 μg/ml of hygromycine for selection of GPIX, GPIbβ, and GPIbα respectively.

### *Measurement for GPIbαβIX expression on CHO cells*

Expression of GPIbα on CHO cells was confirmed by flowcytometry analysis with either the anti-GPIbα antibody, LJ-P3, or the anti-GPIX antibody, SZ1 (Immunotech,

Marseille, France), which reacts with the GPIbIX complex, but does not react with GPIb or GPIX alone. Four types of cells were independently sorted by fluorescence activated cell sorter (FACS) analysis using SZ1. Subsequently, quantitation of GPIbα on each cell was performed using an enzyme immunosorbent assay (EIA) with a glycocalicine EIA kit using GUR83–35 and GUR20–5, according to the supplied protocol. Purified glycocalicine of GPIbα (Lopez, 1994), which has a GPIbα extracytoplasmic domain that contains sites for the $^{145}$Thr/Met and VNTR polymorphisms, was used as a standard in this assay.

### *Perfusion studies: analyses for the interaction of GPIbαβIX-expressing CHO cells with immobilized VWF under flow conditions*

Glass cover slips were incubated with 10 μg/ml of VWF at 4°C overnight and then blocked with 0·5% bovine serum albumin (BSA) (Sigma-Aldrich, Tokyo, Japan) at room temperature for 1 h. CHO cells were harvested with 0·5 mmol/l EDTA, washed twice with phosphate buffered saline, and resuspended in 0·5 mmol/l EDTA/HEPES-Tyrode's buffer without $Ca^{2+}$ and $Mg^{2+}$ to a final concentration of $2 \times 10^5$/ml. The interaction between $10^6$ cells expressing GPIbαβIX and immobilized VWF was examined using a recirculating flow chamber system (Nishiya *et al*, 2000). Cells interacting with the surface were monitored for a 4-min period. Data were stored on video tape. Single-frame video images were analysed using an image processor, an Argus 50 image processor (Hamamatsu Photonics, Hamamatsu, Japan), and rolling velocities of the cells were analysed using an image processor, an Argus 20 image processor (Hamamatsu Photonics). Rolling velocity was determined as the distance cells rolled per second. To confirm the specificity of the cell rolling, experiments under flow conditions were performed in the presence of 10 μg/ml of soluble-VWF or after incubation with 50 μg/ml of anti-GPIbα antibody GUR83–35 at room temperature for 15 min.

### *Statistics*

Differences in immunologic reactivity between 145T and 145M were assessed using Student's *t*-test. Analysis of covariance (ANCOVA) was used to compare the influence of three variables, GPIbα sequence (145T vs. 145M), VWF binding, and day of the experiment, in VWF binding between 145T and 145M. Analysis of variance (ANOVA) was used for analysis of GPIbα expression on CHO cells and the perfusion studies among four types of GPIbα-expressing cells. The Bonferroni *post hoc* test for multiple comparisons was performed to compare the rolling velocity among the cells. ANCOVA was used to analyse three variables; GPIbα sequence (T1R vs M4R), rolling velocity, and day of experiment. A *P*-value of less than 0·05 was considered to be statistically significant.

## Results

### *Comparison of immunologic reactivity of recombinant GPIbα fragments*

To characterize the $^{145}$Thr/Met polymorphism, we established stable cell lines that secreted recombinant GPIbα fragments ($^{1}$His–$^{302}$Ala), 145T or 145M, into the culture medium. The secretion of each fragment into the culture medium was confirmed by Western blot analysis using the LJ-Ibα1 antibody under reduced conditions. An LJ-Ibα1-positive species with a molecular mass of approximately 45-kDa was observed in 145T and 145M, but not in the culture medium from mock-transfected cells. Subsequently, we quantified each fragment by dot-blot analysis with LJ-Ibα1 under reduced conditions. There was similar immunologic reactivity to LJ-Ibα1 between 145T and 145M. An equivalent amount of each fragment was tested in dot-blot analysis for their immunologic reactivity to several anti-GPIbα monoclonal antibodies that recognize confirmation-specific epitopes within the 45-kDa domain and $^{125}$I-anti mouse IgG as a secondary antibody. The binding of each antibody, as measured by counts per minute, was not significantly different between 145T and 145M (Table I), suggesting that the $^{145}$Thr/Met polymorphism does not affect immunologic reactivity for LJ-P3, GUR20–5, and GUR83–35. Similar results by dot-blot analysis using the ECL detection system with anti-mouse IgG antibody as a secondary antibody were observed in seven independent experiments (data not shown).

### *Ristocetin-induced $^{125}$I-labelled VWF binding to immobilized recombinant GPIbα fragments*

To elucidate the effect of the $^{145}$Thr/Met polymorphism on VWF binding, we performed an experiment using recombinant GPIbα fragments without the VNTR polymorphism site, containing residues 1–302. This binding was examined in the absence or presence of ristocetin under static conditions (Fig 1). The binding levels (pmol/well; mean ± SD) were 0·011 ± 0·005 for BSA, 0·018 ± 0·008 for 145T, and 0·016 ± 0·004 for 145M in the absence of ristocetin, indicating no specific binding in this experimental condition. In the presence of ristocetin, specific $^{125}$I-VWF binding was observed in 145T and 145M, but not BSA; 0·015 ± 0·008 for BSA, 0·039 ± 0·015 for 145T, and

**Table I.** Immunologic reactivity (cpm count) in dot-blot analysis.

| | 145T | 145M | *P*-value |
|---|---|---|---|
| LJ-Ibα1 | 2594·0 ± 17·0 | 2536·0 ± 130·1 | 0·5957 |
| LJ-P3 | 2532·0 ± 93·3 | 2771·0 ± 168·3 | 0·2211 |
| GUR20–5 | 2777·0 ± 75·0 | 2730·0 ± 435·6 | 0·8943 |
| GUR83–35 | 2930·0 ± 45·3 | 2622·0 ± 260·2 | 0·2409 |

Values are mean ± SD of duplicate determinations in one experiment.

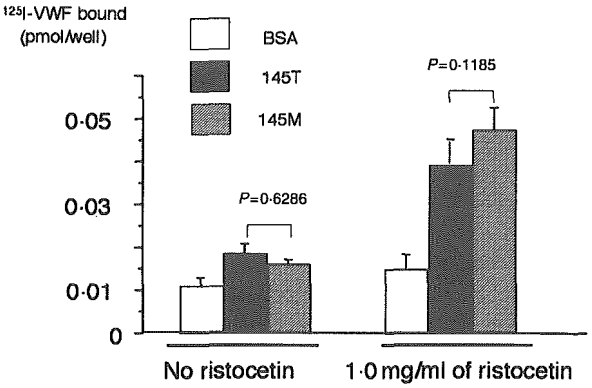


**Fig 1.** Binding of ristocetin-induced $^{125}$I-labelled soluble VWF to immobilized recombinant GPIbα fragment was analysed on nitrocellulose membrane. Membrane-bound radioactivity was counted to assess the binding. BSA was used as a control. Results are mean value ± SD (pmol/well) of duplicates of three independent experiments. Error bars indicate SDs.

0·047 ± 0·017 for 145M, and the binding levels were not different between 145T and 145M ($P = 0·1185$).

To evaluate the binding affinities of 145T and 145M, a Scatchard plot analysis was performed in the presence of 1·0 mg/ml of ristocetin. Both samples had saturable binding of $^{125}$I-VWF, and the dissociation constants (nmol/l; mean ± SD) were 620·5 ± 176·1 for 145T and 406·0 ± 40·2 for 145M ($P = 0·0551$). The maximum number of binding sites ($B_{max}$, nmol/l; mean ± SD) was 68·0 ± 11·4 for 145T and 56·1 ± 11·3 for 145M ($P = 0·1889$). These results suggest that 145T and 145M have a similar binding affinity for VWF in the presence of ristocetin.

### *Quantitation of GPIbα expression on the GPIbβIX-expressing CHO cells*

We prepared four types of GPIbαβIX-expressing CHO cells; two naturally occurring sequences, T1R and M4R, and two artificial or extremely rare sequences, T4R and M1R, to investigate which GPIbα polymorphisms affect the interaction with VWF under flow conditions. First, the surface density of the GPIbαβIX complex on each cell was examined by flowcytometry analysis with LJ-P3 or SZ-1, and the reactivity was not different among cells. Subsequently, four types of GPIbαβIX-expressing CHO cells were isolated using FACS to obtain cells with an equivalent amount of the GPIbαβIX complex on the surface. Moreover, quantitative determination of each sorted cell was performed by EIA using the anti-GPIbα antibodies, GUR83–35 and GUR20–5. The GPIbα expression levels, calculated by standard curves for absorbance and glycocalicine as a standard protein, are shown in Table II. There was no statistically significant difference in the GPIbα expression levels among the four types of cells, although T4R had a slightly higher expression level.

**Table II.** GPIbα molecule on single CHO cell.

| GPIbα sequence | GPIbα molecule (×10$^6$) | *P*-value |
|---|---|---|
| T1R | 4·26 ± 0·31 | 0·1279 |
| M1R | 4·46 ± 0·34 | |
| T4R | 5·26 ± 0·48 | |
| M4R | 4·36 ± 0·17 | |

Values are mean ± SD of duplicate determinations in three independent experiments.

### *Interaction between immobilized VWF and CHO cells expressing the GPIbαβIX complex under flow conditions*

To determine the optimal shear condition, preliminary studies were performed using T1R cells to monitor the interaction between immobilized VWF and GPIbα-expressing CHO cells. Rolling cells per unit area (mm$^2$) of VWF-immobilized glass were counted under various shear conditions. The number of rolling cells was 26·91, 16·34, 8·65, 0·96, and 0 for shear conditions of 32/s, 64/s, 114/s, 214/s, and 600/s respectively. In CHO cells without GPIbα, the rolling cell number was 3·84, 0·96, 0, 0, and 0 for shear conditions of 32/s, 64/s, 114/s, 214/s, and 600/s respectively. We then examined the effect of the anti-GPIbα antibody GUR83–35 on rolling cell number per minute and rolling velocity. Under a shear condition of 32/s, the number of rolling cells per minute was 14 and 16 in the absence and presence of GUR83–35 respectively. Under a shear condition of 114/s, the number was 134 and 41 in the absence and presence of GUR83–35 respectively. The rolling velocity under a shear condition of 32/s was similar between the two experimental conditions; 240·61 ± 67·49 (μm/s, mean ± SD) in the absence of GUR83–35 and 291·98 ± 60·92 in the presence of GUR83–35. In contrast, the rolling velocity under a shear condition of 114/s was different in the absence and presence of GUR83–35; 704·74 ± 153·5 and 959·10 ± 172·1 respectively. These findings indicated that the observed interaction was specific for GPIbα under a shear condition of 114/s, but not of 32/s. Thus, we adopted the shear condition of 114/s for the subsequent experiments.

As shown in Fig 2 and Table III, the rolling velocity of M4R under shear conditions of 114/s was significantly slower than that of T1R ($P = 0·00042$). The rolling velocities of M1R and T4R were similar, with values that were intermediate between those for T1R and M4R. Moreover, we analysed the rolling velocity between T1R and M4R by ANCOVA to test whether the difference identified by ANOVA was affected by different day of experiment. The rolling velocity was 1077·7 ± 20·9 (mean ± SD) for T1R and 918·4 ± 17·3 for M4R ($P < 0·0001$), indicating that the significant difference between T1R and M4R was not influenced by interactions with other variables among the four independent experiments. The number of rolling cells interacting with the immobilized VWF per minute was 32·0 ± 5·6 for T1R, 34·7 ± 2·1 for M1R, 26·7 ± 3·1 for T4R, and 35·7 ± 2·5 for M4R. These values were not significantly different among the four types of cells


 

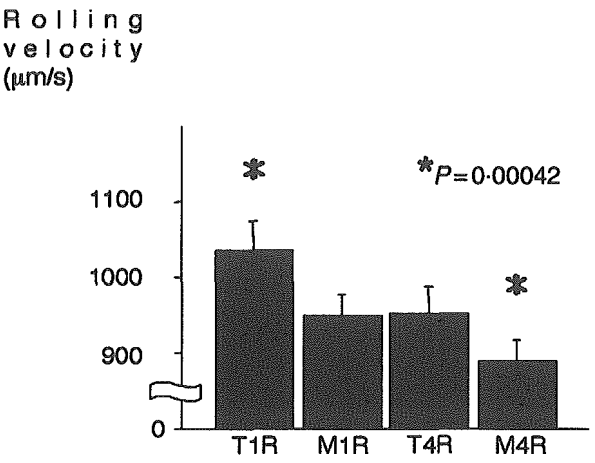


Fig 2. Interaction between immobilized VWF and CHO cells expressing GPIbαβIX complex was analysed under flow conditions (114/s). Each cell sequenced for the GPIbα polymorphism was applied to the flow chamber system with VWF-immobilized glass. Error bars indicate SDs. Results are mean value ± SD (μm/s) of four independent experiments.

($P = 0{\cdot}0574$). In GPIbβIX-expressing CHO cells, the rolling cell number was 5·2 ± 0·5. Under this flow condition, the cell rolling velocity was inhibited by GUR83–35; i.e. the velocities became faster and with soluble-VWF addition (Table III). Thus, the specificity of interaction between immobilized VWF and GPIbα-expressing CHO cells was confirmed under a shear condition of 114/s.

## Discussion

The present study demonstrated that the $^{145}$Met and 4R polymorphisms of GPIbα facilitate interaction with immobilized VWF under flow conditions, which is a highly adaptive physiologic response. To date, molecular mechanisms for the functional differences of the $^{145}$Thr/Met and/or VNTR polymorphisms in GPIbα have not been fully understood whereas numerous epidemiologic data have been reported. We report the first experimental data obtained using recombinant proteins to determine the functional differences of $^{145}$Thr/Met and VNTR GPIbα polymorphisms. Previously, $^{145}$Met and/or 3R/4R polymorphisms were demonstrated to be associated with an increased risk for arterial thrombosis, such as coronary artery disease or stroke (Simmonds *et al*, 2001; Yamada *et al*, 2002). Because the $^{145}$Thr/Met and VNTR polymorphisms are in linkage disequilibrium, focus on either $^{145}$Met or 3R/4R allele was likely to be sufficient to examine the association between GPIbα polymorphisms and arterial thrombosis in the epidemiological study. We reported that the frequency of either $^{145}$Met- or 4R-allele among patients with coronary artery disease was higher than that among control subjects and that the genotypes with the $^{145}$Met-allele were more frequently found in the patients with cerebrovascular disease than in control subjects (Murata *et al*, 1997; Sonoda *et al*, 2000). A large case-cohort study (Afshar-Kharghan *et al*, 2004) showed the relationship of the 2R/2R genotype with a lower risk of coronary heart disease in African-Americans. However, conflicting data have also been published (Hato *et al*, 1997; Simmonds *et al*, 2001). In experimental studies of these polymorphisms, Boncler *et al* (2002) demonstrated that the inhibitory effect of the VWF antagonist on ristocetin-induced agglutination was higher in $^{145}$Met/3R-positive platelets than in $^{145}$Met/3R-negative platelets. Ulrichts *et al* (2003) reported that platelets with $^{145}$Thr or recombinant GPIbα (residues 1–289) with $^{145}$Thr had a higher VWF binding affinity than $^{145}$Met. These findings are not consistent with our results although the experimental conditions of the present study differed from those of previous studies: use of ristocetin or botrocetin or use of an assay system. Other studies have also used various methods with inconsistent results (Mazzucato *et al*, 1996; Li *et al*, 2000; Jilma-Stohlawetz *et al*, 2003). These reports suggest that the functional analyses of GPIbα polymorphisms seem to be easily affected by several factors in relation to platelet activation or experimental conditions. Therefore, in this study, recombinant GPIbα and purified human VWF were examined under two experimental conditions to focus on the relationship between GPIbα polymorphisms and interactions with VWF. The first study, using soluble GPIbα lacking the VNTR polymorphism site, did not show the effect of the $^{145}$Thr/Met polymorphism on the major conformation because the immunoreactivity to anti-GPIbα antibodies that recognize confirmation-specific epitopes were not significantly different between these polymorphisms. The $^{145}$Thr/Met polymorphism did not affect the $^{125}$I-VWF binding in the presence of ristocetin under static conditions. Although ristocetin provides a

Table III. Rolling velocity for GPIbα-expressing cells interacting with VWF under 114/s flow condition

| | Soluble VWF (−) | | | | Soluble VWF (+) | |
|---|---|---|---|---|---|---|
| | GUR83-35 (−) | *P*-value | GUR83-35 (+) | *P*-value | GUR83-35 (−) | *P*-value |
| T1R | 1035·1 ± 40·5* | | 1291·1 ± 61·9 | NS | 1385·7 ± 82·5 | NS |
| M1R | 951·1 ± 26·4** | *0·00042 | 1486·8 ± 109·5 | | 1165·4 ± 62·9 | |
| T4R | 952·5 ± 36·9** | **NS | 1638·9 ± 384·6 | | 1276·6 ± 86·5 | |
| M4R | 902·2 ± 30·8* | | 1521·5 ± 86·6 | | 1293·5 ± 126·4 | |

Values for rolling velocity (μm/s) are mean ± SD. NS, not significant.

convenient method to investigate the VWF/GPIbα interaction *in vitro*, it is not a physiologic substance. Thus, the second study was designed with an alternative approach, an *in vitro* assay for VWF/GPIbα interaction under flow conditions. Cells expressing GPIbα were prepared as a GPIbαβIX complex because expression of a full-length GPIbα alone was unstable in the cell culture system (Lopez *et al*, 1992). Two types of cells with naturally occurring sequences (T1R and M4R) and two types of cells with artificial or extremely rare sequences (T4R and M1R) were used to determine which polymorphism was more closely related to the VWF/GPIbα interaction. We carefully measured the GPIbα expression level on each cell because these levels were reported to affect the VWF/GPIbα interaction under flow conditions (Nishiya *et al*, 2000). After using FACS to obtain cells expressing similar GPIbα levels, EIA assay was performed using GUR83–35 and GUR20–5. Because these two antibodies were shown not to be influenced by the $^{145}$Thr/Met polymorphism (Table I), we used these antibodies in this assay. Perfusion analyses of the quantified cells indicated that M4R, which is a risk factor for arterial thrombosis, had a high ability to interact with VWF under a flow condition of 114/s, as compared with T1R. This flow condition of 114/s may correspond to wall shear rate for large veins *in vivo* (Bevan *et al*, 1995), where VWF-dependent platelet phenomena may not take place. Compared with platelets, however, CHO cells have 2·5- to threefold larger diameters, and the GPIbα-expressing CHO cells are approximately 20-fold higher in GPIbα density. The cell size and receptor density are likely to affect the sensitivity of cells to flow conditions. Also, we were unable to determine the order of effectiveness of the polymorphisms among the four sequences, $^{145}$Thr, $^{145}$Met, 1R, and 4R, in VWF/GPIbα interactions because T4R and M1R had a similar ability to interact with VWF. Although the synergistic effect of the $^{145}$Thr/Met and VNTR polymorphisms on GPIbα function remains unclear, the present data are compatible with previous speculations (Lopez, 1994; Murata *et al*, 1997) that GPIbα with 4R is longer in size and thus places the VWF-binding global domain further away from the platelet plasma membrane. Thus, VWF would be more easily accessible to the binding site on the receptor under high shear conditions. Functional polymorphisms of GPIbα might be responsible for the increased prevalence of arterial thrombosis. Our observations might explain the molecular basis for the previous epidemiologic studies. Further studies to examine the interactions between GPIbα polymorphisms and other ligands are necessary. The present data support a potentially new therapeutic approach to arterial thrombosis by targeting specific GPIbα polymorphisms.

## References


Afshar-Kharghan, V., Matijevic-Aleksic, N., Ahn, C., Boerwinkle, E., Wu, K.K. & Lopez, J.A. (2004) The variable number of tandem repeat polymorphism of platelet glycoprotein Ibalpha and risk of coronary heart disease. *Blood*, **103**, 963–965.

Andrews, R.K., Gardiner, E.E., Shen, Y., Whisstock, J.C. & Berndt, M.C. (2003) Glycoprotein Ib-IX-V. *International Journal of Biochemistry and Cell Biology*, **35**, 357–364.

Bevan, J.A., Kaley, G. & Rubanyi, G.M. (1995) *Flow-Dependent Regulation of Vascular Function*. Oxford University Press, Oxford.

Boncler, M.A., Golanski, J., Paczuski, R. & Watala, C. (2002) Polymorphisms of glycoprotein Ib affect the inhibition by aurintricarboxylic acid of the von Willebrand factor dependent platelet aggregation. *Journal of Molecular Medicine*, **80**, 796–801.

Clemetson, K.J. (1997) Platelet GPIb-V-IX complex. *Thrombosis and Haemostasis*, **78**, 266–270.

Dopheide, S.M., Yap, C.L. & Jackson, S.P. (2001) Dynamic aspects of platelet adhesion under flow. *Clinical and Experimental Pharmacology and Physiology*, **28**, 355–363.

Fraker, P.J. & Speck, J.C., Jr (1978) Protein and cell membrane iodinations with a sparingly soluble chloroamide,1,3,4,6-tetrachloro-3a,6a-diphrenylglycoluril. *Biochemical and Biophysical Research Communications*, **80**, 849–857.

Handa, M., Titani, K., Holland, L.Z., Roberts, J.R. & Ruggeri, Z.M. (1986) The von Willebrand factor-binding domain of platelet membrane glycoprotein Ib. Characterization by monoclonal antibodies and partial amino acid sequence analysis of proteolytic fragments. *Journal of Biological Chemistry*, **261**, 12579–12585.

Hato, T., Minamoto, Y., Fukuyama, T. & Fujita, S. (1997) Polymorphisms of HPA-1 through 6 on platelet membrane glycoprotein receptors are not a genetic risk factor for myocardial infarction in the Japanese population. *American Journal of Cardiology*, **80**, 1222–1224.

Huizinga, E.G., Tsuji, S., Romijn, R.A., Schiphorst, M.E., de Groot, P.G., Sixma, J.J. & Gros, P. (2002) Structures of glycoprotein Ibalpha and its complex with von Willebrand factor A1 domain. *Science*, **297**, 1176–1179.

Ikeda, Y., Murata, M. & Goto, S. (1997) Von Willebrand factor-dependent shear-induced platelet aggregation: basic mechanisms and clinical implications. *Annals of the New York Academy of Sciences*, **811**, 325–336.

Ikeda, Y., Handa, M., Murata, M. & Goto, S. (2000) A new approach to antiplatelet therapy: inhibitor of GPIb/V/IX-vWF interaction. *Haemostasis*, **30** (Suppl.), 44–52.

Ishida, F., Saji, H., Maruya, E. & Furihata, K. (1991) Human platelet-specific antigen, Siba, is associated with the molecular weight polymorphism of glycoprotein Ib alpha. *Blood*, **78**, 1722–1729.

Ishida, F., Furihata, K., Ishida, K., Kodaira, H., Han, K.S., Liu, D.Z., Kitano, K. & Kiyosawa, K. (1996) The largest isoform of platelet membrane glycoprotein Ib alpha is commonly distributed in eastern Asian populations. *Thrombosis and Haemostasis*, **76**, 245–247.

Jilma-Stohlawetz, P., Homoncik, M., Jilma, B., Knechtelsdorfer, M., Unger, P., Mannhalter, C., Santoso, S. & Panzer, S. (2003) Glycoprotein Ib polymorphisms influence platelet plug formation under high shear rates. *British Journal of Haematology*, **120**, 652–655.

Kawasaki, T., Taniuchi, Y., Hisamichi, N., Fujimura, Y., Suzuki, M., Titani, K., Sakai, Y., Kaku, S., Satoh, N., Takenaka, T., Handa, M. & Sawai, Y. (1995) Tokaracetin, a new platelet antagonist that binds to platelet glycoprotein Ib and inhibits von Willebrand factor-dependent shear-induced platelet aggregation. *Biochemical Journal*, **308**, 947–953.

Li, C.Q., Garner, S.F., Davies, J., Smethurst, P.A., Wardell, M.R. & Ouwehand, W.H. (2000) Threonine-145/methionine-145 variants of baculovirus produced recombinant ligand binding domain of

GPIbalpha express HPA-2 epitopes and show equal binding of von Willebrand factor. *Blood*, **95**, 205–211.

Lopez, J.A. (1994) The platelet glycoprotein Ib-IX complex. *Blood Coagulation and Fibrinolysis*, **5**, 97–119.

Lopez, J.A., Leung, B., Reynolds, C.C., Li, C.Q. & Fox, J.E. (1992) Efficient plasma membrane expression of a functional platelet glycoprotein Ib-IX complex requires the presence of its three subunits. *Journal of Biological Chemistry*, **267**, 12851–12859.

Mazzucato, M., Pradella, P., de Angelis, V., Steffan, A. & de Marco, L. (1996) Frequency and functional relevance of genetic threonine145/methionine145 dimorphism in platelet glycoprotein Ib alpha in an Italian population. *Transfusion*, **36**, 891–894.

Moriki, T., Murata, M., Kitaguchi, T., Ambo, H., Handa, M., Watanabe, K., Takahashi, H. & Ikeda, Y. (1997) Expression and functional characterization of an abnormal platelet membrane glycoprotein Ib alpha (Met239 → Val) reported in patients with platelet-type von Willebrand disease. *Blood*, **90**, 698–705.

Moroi, M., Jung, S.M. & Yoshida, N. (1984) Genetic polymorphism of platelet glycoprotein Ib. *Blood*, **64**, 622–629.

Murata, M., Ware, J. & Ruggeri, Z.M. (1991) Site-directed mutagenesis of a soluble recombinant fragment of platelet glycoprotein Ib alpha demonstrating negatively charged residues involved in von Willebrand factor binding. *Journal of Biological Chemistry*, **266**, 15474–15480.

Murata, M., Furihata, K., Ishida, F., Russell, S.R., Ware, J. & Ruggeri, Z.M. (1992) Genetic and structural characterization of an amino acid dimorphism in glycoprotein Ib alpha involved in platelet transfusion refractoriness. *Blood*, **79**, 3086–3090.

Murata, M., Matsubara, Y., Kawano, K., Zama, T., Aoki, N., Yoshino, H., Watanabe, G., Ishikawa, K. & Ikeda, Y. (1997) Coronary artery disease and polymorphisms in a receptor mediating shear stress-dependent platelet activation. *Circulation*, **96**, 3281–3286.

Nishiya, T., Murata, M., Handa, M. & Ikeda, Y. (2000) Targeting of liposomes carrying recombinant fragments of platelet membrane glycoprotein Ibalpha to immobilized von Willebrand factor under flow conditions. *Biochemical and Biophysical Research Communications*, **270**, 755–760.

Ruggeri, Z.M. (2003) von Willebrand factor, platelets and endothelial cell interactions. *Journal of Thrombosis and Haemostasis*, **1**, 1335–1342.

Simmonds, R.E., Hermida, J., Rezende, S.M. & Lane, D.A. (2001) Haemostatic genetic risk factors in arterial thrombosis. *Thrombosis and Haemostasis*, **86**, 374–385.

Simsek, S., Bleeker, P.M., van der Schoot, C.E. & von dem Borne, A.E. (1994) Association of a variable number of tandem repeats (VNTR) in glycoprotein Ib alpha and HPA-2 alloantigens. *Thrombosis and Haemostasis*, **72**, 757–761.

Sonoda, A., Murata, M., Ito, D., Tanahashi, N., Ohta, A., Tada, Y., Takeshita, E., Yoshida, T., Saito, I., Yamamoto, M., Ikeda, Y., Fukuuchi, Y. & Watanabe, K. (2000) Association between platelet glycoprotein Ibalpha genotype and ischemic cerebrovascular disease. *Stroke*, **31**, 493–497.

Suzuki, K., Hayashi, T., Akiba, J., Satoh, S. & Kato, T. (1999) Phenotypic consequence of the gene abnormality in the platelet glycoprotein IX gene observed in a patient with Bernard-Soulier syndrome through mammalian cell expression system. *Thrombosis Research*, **95**, 295–302.

Titani, K., Takio, K., Handa, M. & Ruggeri, Z.M. (1987) Amino acid sequence of the von Willebrand factor-binding domain of platelet membrane glycoprotein Ib. *Proceedings of the National Academy of Sciences of the United States of America*, **84**, 5610–5614.

Uff, S., Clemetson, J.M., Harrison, T., Clemetson, K.J. & Emsley, J. (2002) Crystal structure of the platelet glycoprotein Ib (alpha) N-terminal domain reveals an unmasking mechanism for receptor activation. *Journal of Biological Chemistry*, **277**, 35657–35663.

Ulrichts, H., Vanhoorelbeke, K., Cauwenberghs, S., Vauterin, S., Kroll, H., Santoso, S. & Deckmyn, H. (2003) von Willebrand factor but not alpha-thrombin binding to platelet glycoprotein Ibalpha is influenced by the HPA-2 polymorphism. *Arteriosclerosis, Thrombosis, and Vascular Biology*, **23**, 1302–1307.

Vicente, V., Kostel, P.J. & Ruggeri, Z.M. (1988) Isolation and functional characterization of the von Willebrand factor-binding domain located between residues $His^{1}$-$Arg^{293}$ of the alpha-chain of glycoprotein Ib. *Journal of Biological Chemistry*, **263**, 18473–18479.

Ware, J. (1998) Molecular analyses of the platelet glycoprotein Ib-IX-V receptor. *Thrombosis and Haemostasis*, **79**, 466–478.

Yamada, Y., Izawa, H., Ichihara, S., Takatsu, F., Ishihara, H., Hirayama, H., Sone, T., Tanaka, M. & Yokota, M. (2002) Prediction of the risk of myocardial infarction from polymorphisms in candidate genes. *New England Journal of Medicine*, **347**, 1916–1923.

# Kupffer Cells Alter Organic Anion Transport Through Multidrug Resistance Protein 2 in the Post–Cold Ischemic Rat Liver

Atsushi Kudo,[1,2] Satoshi Kashiwagi,[3] Mayumi Kajimura,[2] Yasunori Yoshimura,[3] Koji Uchida,[4] Shigeki Arii,[1] and Makoto Suematsu[2]

**Although Kupffer cells (KCs) may play a crucial role in post–cold ischemic hepatocellular injury, their role in nonnecrotic graft dysfunction remains unknown. This study examined reveal the role of KC in post–cold ischemic liver grafts. Rat livers treated with or without liposome-encapsulated dichloromethylene diphosphonate, a KC-depleting reagent, were stored in University of Wisconsin (UW) solution at 4°C for 8 to 24 hours and reperfused while monitoring biliary output and constituents. The ability of hepatocytes to excrete bile was assessed through laser-confocal microfluorography *in situ*. Cold ischemia-reperfused grafts decreased their bile output significantly at 8 hours without any notable cell injury. This event coincided with impaired excretion of glutathione and bilirubin-IX$\alpha$ (BR-IX$\alpha$), suggesting delayed transport of these organic anions. We examined whether intracellular relocalization of multidrug resistance protein-2 (Mrp2) occurred. Kinetic analyses for biliary excretion of carboxyfluorescein, a fluoroprobe excreted through this transporter, revealed significant delay of dye excretion from hepatocytes into bile canaliculi. The KC-depleting treatment significantly attenuated this decline in biliary anion transport mediated through Mrp2 in the 8-hour cold ischemic grafts via redistribution of Mrp2 from the cytoplasm to the canalicular membrane. Furthermore, thromboxane $A_2$ ($TXA_2$) synthase in KC appeared involved as blocking this enzyme improved 5-carboxyfluorescein excretion while cytoplasmic internalization of Mrp2 disappeared in the KC-depleting grafts. In conclusion, KC activation is an important determinant of nonnecrotic hepatocellular dysfunction, jeopardizing homeostasis of the detoxification capacity and organic anion metabolism of the post–cold ischemic grafts.** (HEPATOLOGY 2004;39:1099–1109.)

*Abbreviations: KC, Kupffer cell; UW solution, University of Wisconsin solution; BR-IX$\alpha$, bilirubin-IX$\alpha$; Mrp2, multidrug resistance protein 2; BC, bile canaliculi; $TXA_2$, thromboxane $A_2$; CF, carboxyfluorescein; ATP, adenosine triphosphate; TX, thromboxane; EHBRs, Eisai hyperbilirubinemia rats; LDD, liposome-encapsulated dichloromethylene diphosphonate; GSH, reduced glutathione; LDH, lactate dehydrogenase; cAMP, cyclic adenosine monophosphate; CFDA, carboxyfluorescein diacetate.*

*From the [1]Department of Hepatobiliary Pancreatic Surgery, School of Medicine, Tokyo Medical and Dental University, Bunkyo-ku, Tokyo, Japan; the Departments of [2]Biochemistry and Integrative Medical Biology and [3]Obstetrics and Gynecology, Keio University, School of Medicine, Tokyo, Japan; and the [4]Department of Food and Biodynamics, Graduate School of Bioagricultural Sciences, Nagoya University, Nagoya, Japan.*

*Received September 24, 2003; accepted December 23, 2003.*

*Supported, in part, by a grant from Keio University, School of Medicine, the 21st Century Center of Excellence Program, and the Leading Project for Biosimulation and Grant-in-Aid for Creative Science Research (13GS0015) from the Ministry of Education, Sciences, and Technology of Japan as well as by Advanced Medical Technology in Health Sciences Research Grants from Ministry of Health and Welfare in Japan.*

*Address reprint requests to: Makoto Suematsu, M.D., Ph.D., Professor and Chair, Department of Biochemistry and Integrative Medical Biology, Keio University, School of Medicine, 35 Shinanomachi, Shinjuku-ku, Tokyo 160-8582, Japan. E-mail: msuem@sc.itc.keio.ac.jp; fax: +81-3-3358-8138.*



*Published online in Wiley InterScience (www.interscience.wiley.com).*

*DOI 10.1002/hep.20104*

Although use of University of Wisconsin (UW) solution has improved mean preservation time for liver transplantation, primary graft nonfunction and initial poor function still persist.[1–3] The clinical incidence of such dysfunction and the resultant lack of graft survival depend on storage time.[1–4] Reperfusion injury is the main cause of graft failure after prolonged cold ischemia.[5–9] During storage, hepatocytes swell and form blebs.[6–8] Upon reperfusion, however, these same changes in the parenchymal cells are restored without leading to irreversible injury.[6–8] On the other hand, sinusoidal endothelial cells lose their viability, and Kupffer cells (KCs) are activated.[6–10] According to previous studies using rat liver grafts stored in UW solution, the critical storage time at which changes in sinusoidal cells occur is longer than 16 hours.[6,7] In these grafts, cells were damaged to cause platelet trapping,[10] fibrin deposition,[11] and leukocyte margination.[12] In grafts stored for a shorter duration, hepatic adenosine triphosphate (ATP) content was reported to be well recovered after reperfusion, suggesting that parenchymal cells are viable.[13,14]

Otherwise, it has not been determined whether hepatocytes lose their functions without displaying irreversible injury and then interfere with the graft function as a whole. Although biliary output, clearance of taurocholate, and bromosulfophtalein have been measured in previous studies,[13–15] these studies failed to demonstrate such functional alterations in hepatocytes even when the storage time was extended to 18 hours.[13] Scant information is available regarding alterations in the ability of the post–cold ischemic grafts to excrete bile constituents. Such indices include the ability of hepatocytes to generate the osmotic driving force for bile formation and to excrete bile salts or organic anions; thus excretion of glutathione and bilirubin could serve as a marker for detecting early hepatocellular changes in the grafts. The ability to excrete organic anions could determine the efficiency of the graft to detoxify xenobiotics and the severity of post–cold ischemic hyperbilirubinemia, a risk factor for allograft dysfunction in clinical transplantation.[2,16]

We examined changes in constituents of bile samples as a function of storage time and revealed impaired excretion of glutathione and bilirubin as an early event on hepatocytes. This event turned out to be the result of cytoplasmic relocalization of multidrug resistance associated protein 2 (Mrp2), an ATP-dependent transporter for biliary excretion of the organic anions. Our results suggest that the function of this transporter is impaired, whereas the grafts apparently maintain their overall energy charges without showing any notable hepatocellular damage. Furthermore, mechanisms for such a change in hepatocytes appear to involve thromboxane (TX) synthesis in KCs from grafts exposed to a relatively short duration of cold ischemia (8 hours).

## Materials and Methods

***Animal Preparation.*** Experimental protocols were approved by the Animal Care Committee of Keio University School of Medicine in accordance with their institutional guidelines. Male Wistar rats (220–260 g, CLEA Japan, Tokyo) and Eisai hyperbilirubinemia rats (EHBRs) (220–260 g, Sankyo Inc., Tokyo) that had been allowed free access to laboratory chow and tap water were fasted 24 hours before experiments. Livers of these rats were perfused *ex vivo* with oxygenated Krebs-Henseleit buffer as the baseline perfusate[17,18] and stored in UW solution at 4°C for desired lengths of time.[14] When necessary, rats were pretreated with an intravenous injection of liposome-encapsulated dichloromethylene diphosphonate (LDD) 24 hours prior to preparation of the *ex vivo* liver perfusion for the cold storage according to our previous studies.[14,19] As described previously, this procedure eliminated KCs almost completely, as judged by immunohistochemistry.[20] After cold storage, the grafts were gently rinsed with a transportal injection of 40 mL of Krebs Ringer solution and perfused with the oxygenated buffer in the presence or absence of sodium taurocholate at 30 μmol/L at a constant flow (32 mL/min) in a single-pass mode.[14,21] For some experiments, either OKY-046, an inhibitor of thromboxane $A_2$ ($TXA_2$) synthase, or indomethacin, an inhibitor of cyclooxygenase, was added in UW solution as well as in the rinse solution at desired concentrations.[22]

***Determination of Bile and Tissue Constituents.*** Bile samples were used to determine concentrations of total bile salts, phospholipids, reduced glutathione (GSH), and bilirubin-IXα (BR-IXα).[23,24] BR-IXα was determined by an enzyme-linked immunosorbent assay using 24G7.[24] This monoclonal antibody can recognize BR-IXα, the terminal heme-degrading product generated specifically through the HO reaction as described earlier.[24,25] Activities of lactate dehydrogenase (LDH) were measured as described earlier.[17] ATP in the liver grafts was determined by the luciferrin–luciferase method as described elsewhere.[14,21] Cyclic adenosine monophosphate (cAMP) in the grafts was determined by an enzyme-linked immunosorbent assay (Biotrak system, Amersham Biosciences, Buckinghamshire, United Kingdom).

***Analyses of Biliary Excretion Rates of Carboxyfluorescein.*** Carboxyfluorescein (CF) is an organic anion *that* is excreted from various cells through Mrp2.[26,27] The ester precursor of this dye, CF diacetate (CFDA) was loaded transportally into the livers at 50 nmol/L for 10 minutes in the presence of 1.5 mmol/L probenecid, a potent inhibitor of Mrp2.[26,28] This reagent can enter hepatocytes and is hydrolyzed by esterase into CF to be excreted into bile.[14,17,29] After the 10-minute CFDA loading, the liver was perfused with the probenecid-free buffer to trigger the excretion of CF into bile. In the cold ischemic groups, the stored grafts were loaded with the CFDA containing buffer for 10 minutes in the presence of probenecid, followed by removal of probenecid and subsequent reperfusion for 50 minutes. Bile samples collected from these preparations were deep-frozen until the fluorescence measurements were made using a 96-well, multichannel fluorescence spectrophotometer. The measurements were performed under epi-illumination at 440 nm, the isosbestic wavelength of the dye, which yields fluorescence at 510 nm without interfering with the pH values of the samples.[26] The concentration of CF in samples was calibrated with known concentrations of CF dissolved in phosphate buffer saline. As seen later in the Results section, CF concentrations appeared to decline exponentially with time. With this assumption, biliary CF

lifetimes were determined as the $T_{1/2}$ of the exponential decay. Thus this method is insensitive to the initial amounts of CF loaded into the perfused liver.

**In Situ *Visualization of Hepatocellular CF Exclusion.*** Liver grafts loaded with CF using the aforementioned protocols were observed through intravital laser confocal microfluorography as described previously.[14,20,30] As shown later in the Results section, CF was notably loaded into hepatocytes in the presence of probenecid. Upon removal of the reagent, the dye was immediately excluded from hepatocytes, excreted into bile canaliculi (BC) to display honeycomb networks, and finally disappeared from the parenchyma. To examine if the dye exclusion depends on Mrp2 function, some grafts were reperfused with the buffer containing 1.5mmol/L probenecid. The laser confocal microfluorographs were captured by an inverted-type microscope (Diaphot 300, Nikon/Sankei, Tokyo, Japan) equipped with an intensified charged-coupled device (CCD) camera (C5810, Hamamatsu Photonics, Hamamatsu, Japan) and multi-pinhole laser confocal processor (CSU-10, Yokogawa Electric Co., Tokyo, Japan). All microfluorographs were digitally processed into 8-bit gray level images. To calibrate the fluorescence intensities, known concentrations of CF were prepared *in vitro* and the images were captured under the identical optical parameters of the camera. Gray levels in hepatocytes were measured by variable square window ($2 \times 2\ \mu m^2$) using a digital image processor.[18,31] At least 10 different hepatocytes in the microscopic fields of interest were analyzed in a single experiment. Assuming that fluorescence intensities measured at the liver surface is identical to those measured in the solution, gray levels were converted to apparent CF concentrations using the calibration line (designated as CFapp).

We also conducted morphometry to examine structural changes in BC networks as an index of hepatocellular damages. As shown later in the Results section, normally functioning hepatocytes were characterized by polygonal CF filling in surrounding BC, while those damaged were judged by partial disappearance of the surrounding BC network. The number of such intact hepatocytes surrounded by complete BC filling by CF was counted in the areas of interest. Approximately 0.05 $mm^2$ of the liver surface was analyzed in a single experiment for such evaluations.

***Immunohistochemical Analyses of Subcellular Mrp2 Distribution.*** To evaluate Mrp2 in hepatocytes of the grafts, the liver samples were fixed, sliced, and stained with monoclonal antibody $M_2$III-6 according to a previous study.[32] The antigen on the sections was visualized using phycoerythrin-conjugated anti-mouse immunoglobulin G and was observed through laser confocal microfluorography at 488 nm as described elsewhere.[20,30] To examine BC localization and hepatocellular internalization of Mrp2, the sections were double-immunostained with a monoclonal antibody against ZO-1, another marker expressed in hepatocellular junction.[33] To determine changes in the protein distribution in a semiquantitative manner, single-stained microfluorographs of Mrp2 were converted as monochrome 8-bit images.[14] The gray levels (1–256) were measured at both cytoplasmic and canalicular domains in individual hepatocytes. At least five different sites for each domain were chosen in a single cell to calculate the relative values of cytoplasmic intensities versus the corresponding canalicular intensities. Such a measurement was made in 40 to 60 hepatocytes in four different grafts to construct histograms of the percentage of cytoplasmic intensities of Mrp2-associated immunoreactivities [defined as %I-Mrp2(cyt/bc)]. The elevation of this index represented an increase in Mrp2 internalization. The histograms were compared with the control grafts and those exposed to cold ischemia with and without the KC-depleting procedure in the presence or absence of the $TXA_2$ synthase inhibitor.

To examine differences in Mrp2 expression in the whole liver grafts among the groups, Western blot analyses were performed using the same monoclonal antibody. We also investigated alterations in oxidative modification of Mrp2 by immunoprecipitating the protein by the antibody $M_2$III-6 to follow Western analyses by an anti-acrolein monoclonal antibody (5F6).[34,35]

***Statistical Analyses.*** The statistical significance of data among different experimental groups was determined by one-way ANOVA and Fischer's multiple comparison test. $P < .05$ was considered significant.

## Results

***Storage Time–Dependent Reduction of Bile Output in Liver Grafts.*** To test the viability of liver grafts, the release of LDH in the venous perfusate was measured as an index of cell lysis. As seen in Table 1, the grafts exposed to cold ischemia for less than 24 hours did not display any notable elevation of LDH. At 48 hours, the LDH release became evident at the beginning and end of the 60-minute reperfusion, showing that necrotic cell death was undetectable in cold ischemic grafts exposed less than 24 hours under the current experimental conditions. Figure 1 illustrates time courses of bile output as a function of reperfusion time in grafts undergoing varied lengths of cold ischemia. As seen in panel A, where sodium taurocholate was added, the grafts exposed to 8-hour ischemia increased their output to a level comparable to that in the controls at 30 minutes, but decreased it 50 to 60 minutes after the initial reperfusion. In the grafts exposed to pro-

**Table 1. Effect of the Duration of Cold Preservation on the Release of LDH in the Venous Perfusate of the Grafts**

| Length of Cold Storage (Hrs) | 5 Min-R | 60 Min-R |
|---|---|---|
| Control | 20 ± 6 | 35 ± 11 |
| 8 | 31 ± 7 | 25 ± 9 |
| 16 | 21 ± 8 | 34 ± 6 |
| 24 | 45 ± 8 | 43 ± 22 |
| 48 | 878 ± 377* | 1206 ± 719* |

Data represent means ± SE of measurements (mIU/min/g liver) from the grafts at the onset (0 min) and 60 min after the start of reperfusion (0-24 hrs; n = 5, 48 hrs; n = 3).

*$P < 0.05$ as compared with the value in other groups.

longed cold ischemia for 16 to 48 hours, such a reduction of output became further evident. Panel B shows the time course of bile recovery monitored in the absence of sodium taurocholate in the perfusate. The groups treated with cold ischemia for longer than 16 hours displayed significant decreases in output.

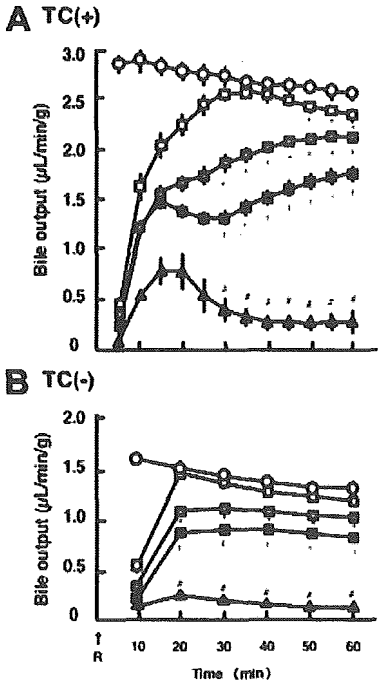


Fig. 1. Time courses of the bile output of liver grafts that have undergone cold preservation followed by reperfusion. Open circles denote the data from nonischemic control livers. Open, shaded, and closed squares indicate the data from grafts exposed to 8-, 16-, and 24-hour cold storage, respectively. Closed triangles indicate the data from 48-hour storage grafts. Values are mean ± SE of five separate experiments. TC (+) and TC (−): data collected in the presence and absence of sodium taurocholate at 30 μmol/L. R: the onset of reperfusion. Note that both bile salt-independent and -dependent outputs were decreased in the 16-hour preserved grafts. *$P < .05$ compared with the data from control. †$P < .05$ compared with the data from 16-hour grafts. #$P < .05$ compared with the data from 24-hour grafts.

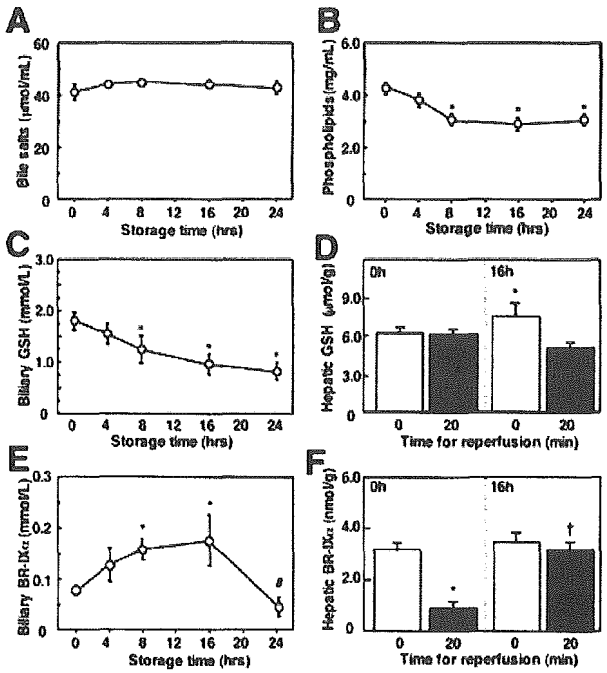


Fig. 2. Effects of duration of cold ischemia on biliary concentrations of bile constituents. Data of bile constituents were collected 20 minutes after the onset of reperfusion. (A) Bile salts. (B) Phospholipids. (C) Concentrations of reduced GSH in bile. (D) Hepatic content of GSH in the control and 16-hour stored grafts measured before and 20 minutes after reperfusion. (E) Concentrations of BR-IXα in bile. (F) Hepatic content of BR-IXα in the control and 16-hour stored grafts measured before and 20 minutes after reperfusion. Values are mean ± SE of five to seven separate experiments. *$P < .05$ compared with the data from control livers. #$P < .05$ compared with the data from the 16-hour group. †$P < .05$ compared with the data from the control grafts exposed to 20-minute reperfusion.

***Alterations in Biliary Excretion of Glutathione and Bilirubin in Post–Cold Ischemic Livers.*** Observation of a significant decrease in bile flow in the grafts undergoing 16- and 24-hour cold ischemia led us to determine which bile constituents were responsible for cholestatic changes. Figure 2 presents data of bile constituents measured 20 minutes after the onset of reperfusion that were plotted as a function of storage time for cold ischemia. Concentrations of bile salts did not exhibit any significant reduction in any length of storage time, while those of phospholipids displayed notable reduction in both concentrations and fluxes in the group exposed to 8- to 24-hour cold ischemia (Fig. 2A, B). Considering that phospholipids are primarily excreted from hepatocytes into biliary compartments, these data suggest the presence of hepatocellular dysfunction in the grafts stored for more than 8 hours.

We next examined biliary excretion of GSH (Fig. 2C). Biliary concentrations in GSH were significantly reduced at 8 hours and declined as a result of the cold storage time.

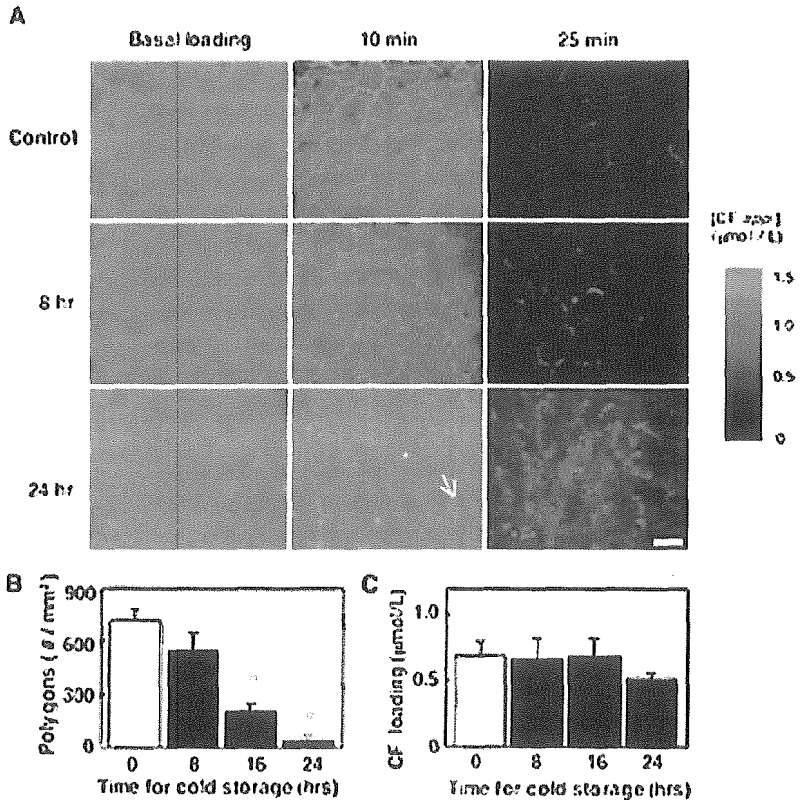


Fig. 3. Alterations in dynamics of hepatocellular CF excretion into BC in cold ischemia–reperfused grafts. (A) Representative pictures of the canalicular CF excretion captured before (Basal loading), and 10 minutes and 25 minutes after removal of probenecid. Note disruption of honeycomb patterns of BC networks in the 24-hour cold ischemic-reperfused graft (**arrow**). Color bar indicates the fluorescence intensities calibrated with known concentrations of CF (bar = 30 $\mu$m). (B) Differences in reperfusion-induced disruption of BC networks as judged by the density of CF-filled polygons in the grafts stored for varied duration of cold ischemia. $^*P < .05$ compared with the data from control livers. (C) Initial hepatocellular CF concentrations showing comparable CF loading among groups. Values are mean ± SE of five separate experiments.

We then examined the hepatic content of GSH; as seen in Fig. 2D, hepatic GSH content did not change before or after 20-minute reperfusion. In the grafts stored for 16 hours, the content apparently increased as a result of the use of UW solution containing GSH; upon 20-minute reperfusion, however, the content was rapidly repressed to the control level as GSH was removed from circulation, showing that the 20-minute reperfusion following 16-hour cold ischemia does not change the basal GSH content in the grafts. These results suggest that the decrease in biliary GSH excretion in the post–cold ischemic livers results from impairment of its transport to bile rather than from its reduction in the grafts, as long as the storage time was less than 16 hours. Because GSH is excreted through Mrp2, we next examined alterations in biliary concentrations of BR-IX$\alpha$, a bile pigment excreted through the same transporter. As seen in Fig. 2E, the biliary concentration of BR-IX$\alpha$ in the initial 20-minute reperfusion was significantly elevated in the 8-hour ischemic group and reached its maximum in the 16-hour storage group. Finally, in the grafts undergoing 24-hour cold ischemia, initial concentrations of BR-IX$\alpha$ were abruptly decreased. Figure 2F illustrates the ability of the grafts to eliminate endogenous BR-IX$\alpha$ into bile. As seen in the control grafts, hepatic content of this bile pigment significantly decreased within the initial 20-minute perfusion. On the other hand, the same duration of reperfusion did not cause such a decrease in the 16-hour treated grafts. These results suggest that the ability of the 16-hour grafts to generate BR-IX$\alpha$ *de novo* surpasses their capacity to excrete the pigment into bile.

***Global and Local Assessment of Mrp2 Function by CF Exclusion.*** Alteration in biliary excretion of GSH and BR-IX$\alpha$ raised the possibility that the ability of Mrp2 to eliminate these organic anions from hepatocytes could be impaired in grafts exposed to prolonged cold ischemia. However, because initial amounts of glutathione and BR-IX$\alpha$ were different among groups, measuring biliary excretion of these endogenous anions did not allow us to make a fair comparison of the organic anion-excreting ability of the grafts. To overcome this difficulty, the grafts were loaded with CF, an exogenous organic anion, and its elimination from hepatocytes into bile was examined. As seen in the left panels of Fig. 3A, hepatocellular CF loading appeared comparable among the grafts exposed to different lengths (0–24 hours) of cold ischemia. This was confirmed by the fluorescence intensitometry in Fig. 3C, indicating that the hepatocytes were viable. This was also consistent with results showing no notable release of LDH (Table 1). Immediately after the removal of probe-

necid, an inhibitor of Mrp2, CF loaded in hepatocytes was rapidly excreted into BC, forming honeycomb networks over the lobule within 10 minutes (Fig. 3A, middle column). At 25 minutes (Fig. 3A, right column), little fluorescence inside the cytoplasm became detectable, if any. In grafts that underwent cold ischemia reperfusion, two major changes in biliary CF excretion occurred: retardation of hepatocellular dye exclusion as judged by an elevation of the basal fluorescence at 25 minutes, and disappearance and deformation of bile canalicular networks as indicated in micrographs collected at 10 minutes. These changes became evident in grafts exposed to extended cold ischemia for 24 hrs (the bottom row in Fig. 3A).

Careful scanning at the site of BC in these microfluorographs captured at 10 minutes showed minimal but notable changes in the structure of the canalicular networks. As seen in Fig. 3B, the number of hepatocytes that were completely surrounded by CF-filled BC decreased as the duration of cold ischemia increased. Such a reduction of polygons became readily apparent in the grafts stored for 16 hours. Because the initial CF loading in hepatocytes was comparable in a range between 0 and 24 hours of ischemic duration, morphologic changes in BC appeared to occur initially at 16-hour cold ischemia. In other words, grafts exposed to 8-hour cold ischemia did not exhibit any significant changes in the morphology of BC networks.

The delay of CF exclusion was further examined in a quantitative manner by monitoring temporal alterations in the fluorescence of the graft hepatocytes (Fig. 4A). When probenecid was perfused continuously, the dye stayed in the cells, exhibiting a slight decline without showing canalicular excretion. As plotted in Fig. 4B, gray levels measured in hepatocytes allowed us to determine the $T_{1/2}$ of the CF exclusion from hepatocytes. Figure 4C illustrates $T_{1/2}$ values among the groups. In the absence of probenecid, $T_{1/2}$ was approximately 6 minutes, while in the presence of probenecid the decay was substantially slowed, suggesting near complete inhibition of Mrp2 transport. $T_{1/2}$ of the 8-hour cold ischemic graft to excrete CF was significantly greater, ranging midway between the control value and that measured in livers of EHBRs. It could be speculated that the smaller $T_{1/2}$ values in this mutant species compared with the probenecid-treated group is due to compensatory excretion of the dye through Mrp3 into the sinusoidal space.[36]

***Effects of KC Depletion on Biliary CF Excretion in 8-hour Cold Ischemic Grafts.*** We attempted to evaluate the ability of the 8-hour cold ischemic grafts as a whole to excrete CF. To this end, the $T_{1/2}$ values for the dye exclusion were determined (Fig. 5). After removal of probenecid ($T_0$ in

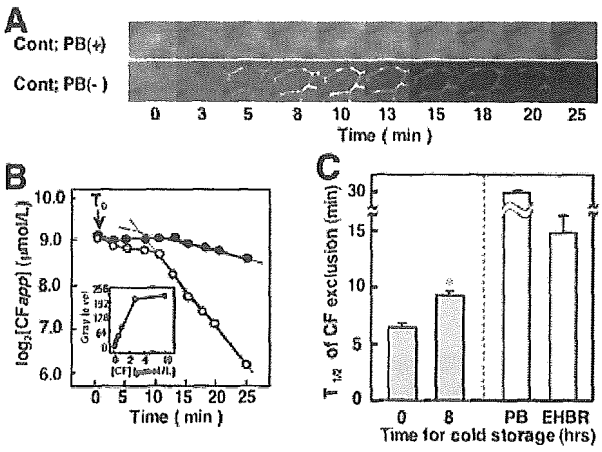


Fig. 4. *In vivo* quantitative analyses of Mrp2 function by visualizing BC excretion of CF. (A) Representative series of pictures showing the dye excretion from individual hepatocytes. Upper section: images from a graft perfused in the presence of 1.5 mM probenecid [PB(+)]. Lower section: images captured after the removal of probenecid [PB(−)]. Note the time-dependent reduction of fluorescence in the cells followed by condensation and disappearance of the dye in surrounding BC. The dye retention in the cells should also be noted. (B) The decay of hepatocellular CF fluorescence. Hepatocellular CF concentrations in the grafts treated with (**closed circles**) or without (**open circles**) probenecid were plotted semilogarithmically against the time so that a straight line represents an exponential curve. Inset: the calibration curve indicating the relationship between concentrations of CF and 8-bit gray levels. [CFapp]: apparent concentrations of CF. CF concentrations were linearly related to gray levels at concentrations less than 3 μmol/L ($r^2 = 0.996$, $P < .05$). (C) Differences in half-life time ($T_{1/2}$) of CF exclusion from hepatocytes. Values are mean ± SE of five separate experiments in each group. $^*P < .05$ compared with the data from control livers. EHBR: grafts isolated from Eisai hyperbilirubinemia rats. PB: grafts perfused with 1.5 mM probenecid.

Fig. 5A), the CF concentrations in bile transiently increased and gradually returned to the basal level. Such a transient increase was not observed either in the presence of probenecid (shaded circles), or in the grafts isolated from EHBRs (closed circles), suggesting that Mrp2 is responsible for biliary CF excretion. When the CF exclusion was analyzed in the whole liver grafts stored for 8 and 16 hours, the decay appeared to be slower than that of the controls. Using the data collected from the 8-hour ischemic grafts, logarythmic values of the CF concentrations versus those at the peak (10 minutes) in bile samples were replotted as a function of reperfusion time (Fig. 5B). The $T_{1/2}$ values of the dye exclusion were then compared between the grafts treated with and without the KC depletion. In the livers untreated with LDD [KC(+)], the 8-hour cold ischemia exhibited prolonged $T_{1/2}$ values compared with the controls. Such a difference in $T_{1/2}$ between the two groups completely disappeared in the KC-depleting grafts. It is noteworthy that in the non–cold ischemic control livers, the KC-depleting procedure by itself did not alter the $T_{1/2}$ values; this indicates that the ameliorating

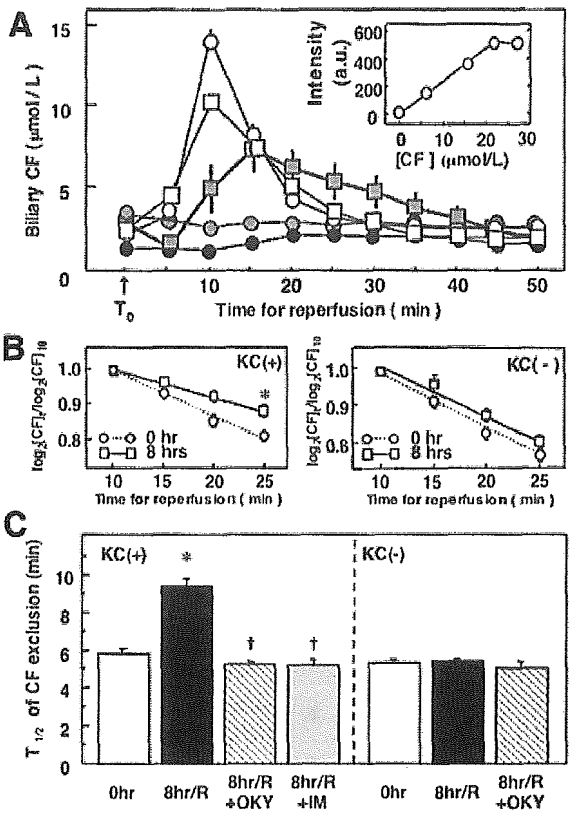


Fig. 5. Alterations in the ability of liver grafts to excrete CF into bile upon cold ischemia reperfusion. (A) Differences in time course of the biliary CF excretion in grafts exposed to varied lengths of cold ischemia. Open circles: control grafts perfused right after removing 1.5 mM probenecid, an Mrp2 inhibitor. Open and shaded squares: grafts undergoing 8- and 24-hour cold storage followed by reperfusion in the absence of probenecid, respectively. Shaded circles: grafts normoperfused in the presence of probenecid. Closed circles: normoperfused grafts isolated from EHBRs. Values are mean ± SE of five separate experiments. $T_0$: time when probenecid was removed from the perfusate. Inset: a linear relationship between the CF concentration and fluorescence intensities. (B) Alterations in relative CF concentrations in bile collected at varied duration of reperfusion and effects of the depletion of KCs. Left: differences in the decay of biliary CF excretion between control (**broken lines**) and 8-hour stored liver grafts (**solid lines**). Right: effects of KC depletion by intravenous LDD. Open circles: control (**broken lines**). Open squares: 8-hour stored grafts (**solid lines**). Data represent mean ± SE of measurement from four separate experiments. *$P < .05$ compared with the decays of CF exclusion in control livers. (C) Effects of KC depletion [KC(−)] by LDD and/or treatment with OKY-046 (OKY), an inhibitor of $TXA_2$ synthase, on lengthening $T_{1/2}$ values in the 8-hour cold storage livers. IM: indomethacin. Concentrations of OKY-046 and indomethacin in the storage and rinse solutions were 240 and 28 μmol/L, respectively. Note that an inhibitory action of OKY-046 disappears in the KC-depleting grafts. Values are mean ± SE of five to six separate experiments. *$P < .05$ compared with the data from control livers. †$P < .05$ compared with the data in the 8-hour stored grafts.

effect of the KC depletion became evident only when the grafts experienced cold ischemia reperfusion.

To reveal mechanisms through which KCs in the 8-hour cold ischemic grafts caused prolonged CF excretion through Mrp2, we examined the involvement of TX, a major prostanoid released from activated KCs under post–cold ischemic conditions.[37,38] To this end, the effects of OKY-046, an inhibitor of $TXA_2$ synthase, were examined. As seen in Fig. 5C, application of this reagent at 240 μmol/L to the storage and rinse solutions abolished an increase in $T_{1/2}$ values of the CF exclusion almost completely. Because the $TXA_2$ synthase inhibitor might increase availability of arachidonic acid to synthesize other prostanoids (*e.g.*, $PGE_2$ and $PGF_{2\alpha}$), we examined if indomethacin, an inhibitor that suppresses all the prostanoids produced via the cyclooxygenase pathway (including TX) could attenuate or aggravate the $T_{1/2}$ values. As shown, this inhibitor also attenuated the prolonged $T_{1/2}$ values almost completely. Furthermore, effects of OKY-046 on the 8-hour cold ischemic grafts disappeared when KC was depleted, suggesting that the involvement of TX is KC-dependent.

***Intracellular Relocalization of Mrp2 by 8-hour Cold Ischemia and Its Attenuation by KC Depletion.*** Because KCs are known to down-regulate Mrp2 in endotoxin-treated livers,[39] we examined if such a change could be involved in the mechanisms for the dysfunction of the transporter. As shown by Western blot analysis, amounts of Mrp2 protein were unchanged in the 8-hour cold ischemic grafts (Fig. 6A) as well as in the 24-hour ischemic grafts (data not shown). We also examined if the protein by itself was oxidatively modified as a consequence of postischemic oxidative insults. However, no apparent changes were found as judged by immunoprecipitation using the anti-acrolein antibody. An examination was then performed to determine whether or not hepatocellular localization of the protein is modified in the 8-hour cold ischemic grafts. As seen in Fig. 6B, its localization in BC was markedly reduced, while the background fluorescence in cytoplasm of hepatocytes was elevated in the 8-hour ischemia-reperfused grafts. As seen in the lower panels of Fig. 6, double-immunostaining with ZO-1 (green) revealed that colocalization of Mrp2 (red) in BC was markedly disrupted, while its intensities in the cytoplasm were elevated, suggesting the internalization of the protein. Such changes were attenuated in the grafts treated with KC depletion or OXY-046. The %I-Mrp2(cyt/bc) values—an index for internalization—indicated that the 8-hour cold ischemia-reperfusion significantly enhanced the Mrp2 internalization and that treatment with KC depletion or with blockade of $TXA_2$ synthase improved BC relocalization of the transporter.

We identified differences in the hepatic contents of ATP and cAMP in the KC(+) and KC(−) grafts after the 8-hour cold ischemia-reperfusion, but there was no notable significance between the two groups (3.4 ± 0.9 vs. 2.9 ± 1.1 μmol/g liver in ATP content and 8.9 ± 1.0 vs. 9.2 ± 0.5 pmol/g liver in cAMP content). These results

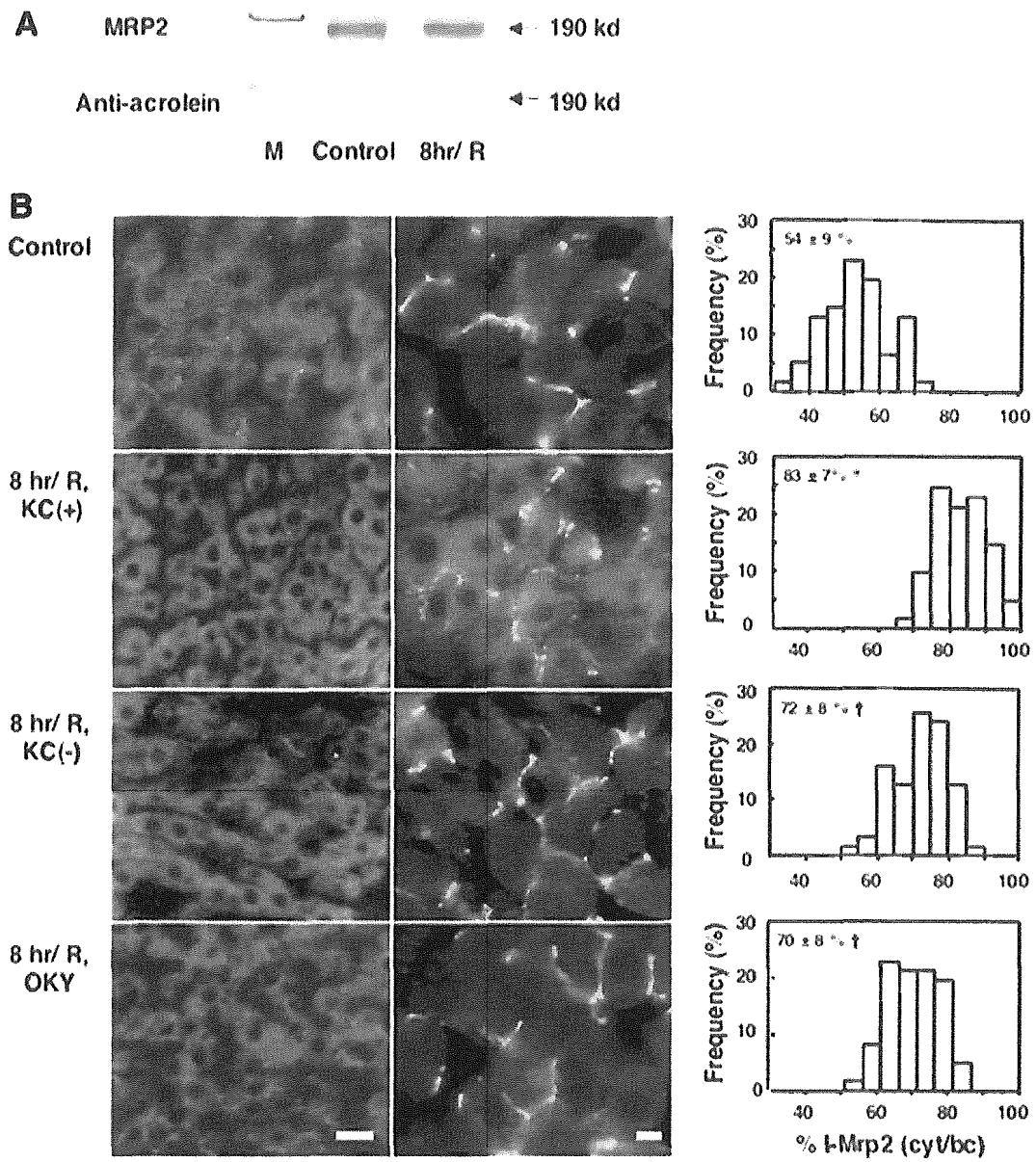


Fig. 6. Disruption of intracellular distribution of Mrp2 in liver grafts exposed to 8-hour cold ischemia and 60-minute reperfusion (8-hour/R), and effects of KC-depleting procedure [KC(−)] or treatment with OKY-046 (OKY). (A) Western blot analysis and immunoprecipitation of Mrp2 by the anti-acrolein monoclonal antibody (5F6). M: molecular marker. (B) Immunofluorescence analysis of Mrp2 distribution. Left: single staining with the anti-Mrp2 monoclonal antibody ($M_2$III-6) labeled with phycoerythrin (bar = 30 $\mu$m). Right: double immunostaining with the FITC-labeled ZO-1 antibody and the phycoerythrin-labeled $M_2$III-6 antibody (bar = 10 $\mu$m). (C) Semiquantitative analyses of hepatocellular Mrp2 localization. %I-Mrp2(cyt/bc); cytoplasmic intensities of Mrp2-associated immunoreactivities versus those measured at BC. Values are mean ± SE of measurements in 40 to 60 hepatocytes/graft from four separate livers. *$P < .05$ compared with the data from control livers. †$P < .05$ compared with the data collected from the 8-hour/R-KC(+) group.

suggest that amelioration of intracellular retrieval of this ATP-binding protein by the KC depletion did not result from alterations in tissue contents of ATP and cAMP.

## Discussion

This study provided evidence that the impaired ability of hepatocytes to carry out the Mrp2-dependent excretion of organic anions is an early event during graft dysfunction caused by cold ischemia, followed by a short duration of reperfusion. This change in hepatocytes was subtle and not associated with necrosis; nevertheless, it was critical enough to cause an imbalance between the cellular generation and excretion of glutathione and bilirubin at the level of the whole graft. Extending the duration of cold

ischemia up to 16 hours induced dysfunction of BC as characterized by their disappearance and dilation, while their polygonal networks were kept intact unless the duration of cold storage exceeded 8 hours. To our knowledge, it remains unknown whether or not such a nonnecrotic dysfunction of hepatocytes exposed to a relatively short period of cold ischemia could be mediated by postischemic responses of sinusoidal cells involving KCs. As this study shows, the reduced ability of hepatocytes to excrete organic anions via Mrp2 was completely restored by depleting KCs, suggesting involvement of these sinusoidal cells in the mechanisms of the dysfunction.

The impairment of Mrp2-mediated transport in the 8-hour post–cold ischemic grafts results from cytoplasmic relocalization of this transporter from canalicular membrane, not from disruption of BC networks or oxidative self-modification of the transporter. This is consistent with our previous observation that 8-hour cold ischemia and reperfusion does not exhibit evidence of oxidative stress in liver grafts.[14] Alterations in cAMP, a determinant for BC sorting of Mrp2,[32,40,41] are unlikely to play a role in the KC-mediated dysfunction, because its content did not differ irrespective of the presence of KCs. Hepatocellular content of ATP is another determinant of transporter function; however, it most likely plays a small role (if any) in the mechanisms, because any differences were not notable between the KC-depleting and control grafts having undergone 8-hour cold ischemia. Because KC depletion did not alter the ability of Mrp2 to excrete organic anions in normal livers, such an alteration of the transporter function in the grafts appears to result from responses of KCs that cannot be triggered unless the graft undergoes cold ischemia reperfusion. Although detailed mechanisms remain unknown, the present results suggest involvement of $TXA_2$ synthase, the enzyme responsible for TXs, a major class of prostanoids released from KCs.[37,38] The observation that the preventive effect of the enzyme inhibitor was completely cancelled in the KC-depleted grafts led us to suggest that KCs constitute a major source of TXs that trigger internalization of Mrp2 into the cytoplasm of hepatocytes. Although $TXA_2$ has been thought to exert potent biologic actions on various types of cells, previous studies provided evidence that $TXB_2$, a relatively stable metabolite of $TXA_2$, is able to activate nonlysosomal proteinases and thereby triggers bleb formation of primary cultured hepatocytes.[42] Thus, further mechanisms by which KC-derived TXs cause hepatocellular dysfunction should be necessary.

The newly developed method of dye exclusion analyses from grafts preloaded with controlled amounts of CF revealed that relocalization of Mrp2 occurs at hepatocellular levels and results in significant deterioration of the whole-graft function. As seen in Fig. 3, the 8-hour storage significantly reduced biliary glutathione excretion without showing any change in tissue content. Because this organic anion serves as the major substance yielding the osmotic driving force for bile acid–independent bile formation, its reduction in bile could result in a decrease in output. This notion is also consistent with our observation that 8-hour stored grafts displayed a significant reduction of output.

In this context, the imbalance between endogenous generation and biliary excretion of BR-IX$\alpha$ in the grafts is of great interest. As seen in Fig. 2, the control liver can excrete approximately 75% of endogenous BR-IX$\alpha$ into bile within 20 minutes of perfusion, which is consistent with our previous studies.[24] On the other hand, such a rapid elimination of bile pigment did not occur in the 16-hour cold ischemic grafts. As judged by biliary concentrations of BR-IX$\alpha$ (Fig. 2E), the absolute amounts of the pigment were elevated but never decreased compared with the non–cold ischemic control grafts. Because amounts of BR-IX$\alpha$ released into circulation were negligible (data not shown), these results suggest that the cold ischemic grafts synthesize greater amounts of the pigment during the initial 20-minute reperfusion than those expected from their capacity to excrete it into bile. This notion is in good agreement with our observation that the graft induces heme oxygenase-1, the stress-inducible enzyme for heme degradation.[43] This event is of pathophysiologic importance with regard to antioxidative stress responses of post–cold ischemic grafts. We have recently reported that low-dose bilirubin can ameliorate oxidative stress and thereby protect post–cold ischemic liver grafts, although it is obviously harmful in excessive doses.[31,43] In the grafts exposed to cold ischemia, reperfusion could cause two important events that critically dictate hepatic bilirubin metabolism: increased heme degradation and decreased excretion of BR-IX$\alpha$ through Mrp2. Thus, combined actions of these two events could result in accumulation of this antioxidant sufficient enough to protect hepatocytes, while their prolonged effects lead to hepatocellular damages and hyperbilirubinemia in the later period of reperfusion.

KCs are potent generators of eicosanoids, while hepatocytes and ATP-binding cassette transporters expressed on their membrane help their degradation and excretion, respectively.[38,39] On the other hand, antioxidant organic anions such as glutathione and bilirubin share Mrp for their excretion into bile in the post–cold ischemic grafts. Thus, the balance between KC-mediated synthesis of eicosanoids and their removal from hepatocytes could determine redistribution of the antioxidant anions in and around hepatocytes, thereby dictating functional out-

come of liver transplantation. KC-mediated remodeling of Mrp-mediated organic anion transport deserves further studies, provided that quantitative information on intra- and intercellular kinetics of glutathione and BR-IXα becomes available. Such studies could answer if KC-yielded TX could serve as an early alert mechanism against subsequent oxidative stress on liver grafts.

## References


1. Ploeg RJ, D'Alessandro AM, Knechtle SJ, Stegall MD, Pirsch JD, Hoffmann RM, Sasaki T, et al. Risk factors for primary dysfunction after liver transplantation—a multivariate analysis. Transplantation 1993;55:807–813.
2. Deschenes M, Belle SH, Krom RA, Zetterman RK, Lake JR. Early allograft dysfunction after liver transplantation: a definition and predictors of outcome. National Institute of Diabetes and Digestive and Kidney Diseases Liver Transplantation Database. Transplantation 1998;66:302–310.
3. Porte RJ, Ploeg RJ, Hansen B, van Bockel JH, Thorogood J, Persijn GG, Hermans J, et al. Long-term graft survival after liver transplantation in the UW era: late effects of cold ischemia and primary dysfunction. European Multicentre Study Group. Transpl Int 1998;11(Suppl 1):S164–S167.
4. Adam R, Bismuth H, Diamond T, Ducot B, Morino M, Astarcioglu I, Johann M, et al. Effect of extended cold ischaemia with UW solution on graft function after liver transplantation. Lancet 1992;340:1373–1376.
5. Jaeschke H. Preservation injury: mechanisms, prevention and consequences. J Hepatol 1996;25:774–780.
6. Caldwell-Kenkel JC, Currin RT, Tanaka Y, Thurman RG, Lemasters JJ. Reperfusion injury to endothelial cells following cold ischemic storage of rat livers. HEPATOLOGY 1989;10:292–299.
7. Caldwell-Kenkel JC, Currin RT, Tanaka Y, Thurman RG, Lemasters JJ. Kupffer cell activation and endothelial cell damage after storage of rat livers: effects of reperfusion. HEPATOLOGY 1991;13:83–95.
8. Lemasters JJ, Thurman RG. Reperfusion injury after liver preservation for transplantation. Annu Rev Pharmacol Toxicol 1997;37:327–338.
9. Clavien PA. Sinusoidal endothelial cell injury during hepatic preservation and reperfusion. HEPATOLOGY 1998;28:281–285.
10. Sindram D, Porte RJ, Hoffman MR, Bentley RC, Clavien PA. Platelets induce sinusoidal endothelial cell apoptosis upon reperfusion of the cold ischemic rat liver. Gastroenterology 2000;118:183–191.
11. Arai M, Mochida S, Ohno A, Fujiwara K. Blood coagulation in the hepatic sinusoids as a contributing factor in liver injury following orthotopic liver transplantation in the rat. Transplantation 1996;62:1398–1401.
12. Clavien PA, Harvey PR, Sanabria JR, Cywes R, Levy GA, Strasberg SM. Lymphocyte adherence in the reperfused rat liver: mechanisms and effects. HEPATOLOGY 1993;17:131–142.
13. Vajdova K, Smrekova R, Mislanova C, Kukan M, Lutterova M. Cold-preservation-induced sensitivity of rat hepatocyte function to rewarming injury and its prevention by short-term reperfusion. HEPATOLOGY 2000; 32:289–296.
14. Kumamoto Y, Suematsu M, Shimazu M, Kato Y, Sano T, Makino N, Hirano KI, et al. Kupffer cell-independent acute hepatocellular oxidative stress and decreased bile formation in post-cold-ischemic rat liver. HEPATOLOGY 1999;30:1454–1463.
15. Imamura H, Brault A, Huet PM. Effects of extended cold preservation and transplantation on the rat liver microcirculation. HEPATOLOGY 1997;25: 664–671.
16. Williams JW, Vera S, Peters TG, Van Voorst S, Britt LG, Dean PJ, Haggitt R, et al. Cholestatic jaundice after hepatic transplantation. A nonimmunologically mediated event. Am J Surg 1986;151:65–70.
17. Suzuki H, Suematsu M, Ishii H, Kato S, Miki H, Mori M, Ishimura Y, et al. Prostaglandin E1 abrogates early reductive stress and zone-specific paradoxical oxidative injury in hypoperfused rat liver. J Clin Invest 1994;93: 155–164.
18. Suematsu M, Goda N, Sano T, Kashiwagi S, Egawa T, Shinoda Y, Ishimura Y. Carbon monoxide: an endogenous modulator of sinusoidal tone in the perfused rat liver. J Clin Invest 1995;96:2431–2437.
19. Kyokane T, Norimizu S, Taniai H, Yamaguchi T, Takeoka S, Tsuchida E, Naito M, et al. Carbon monoxide from heme catabolism protects against hepatobiliary dysfunction in endotoxin-treated rat liver. Gastroenterology 2001;120:1227–1240.
20. Goda N, Suzuki K, Naito M, Takeoka S, Tsuchida E, Ishimura Y, Tamatani T, et al. Distribution of heme oxygenase isoforms in rat liver. Topographic basis for carbon monoxide-mediated microvascular relaxation. J Clin Invest 1998;101:604–612.
21. Shiomi M, Wakabayashi Y, Sano T, Shinoda Y, Nimura Y, Ishimura Y, Suematsu M. Nitric oxide suppression reversibly attenuates mitochondrial dysfunction and cholestasis in endotoxemic rat liver. HEPATOLOGY 1998; 27:108–115.
22. Ishiguro S, Arii S, Monden K, Fujita S, Nakamura T, Niwano M, Harada T, et al. Involvement of thromboxane $A_2$-thromboxane $A_2$ receptor system of the hepatic sinusoid in pathogenesis of cold preservation/reperfusion injury in the rat liver graft. Transplantation 1995;59:957–961.
23. Jaeschke H, Smith CV, Mitchell JR. Reactive oxygen species during ischemia-reflow injury in isolated perfused rat liver. J Clin Invest 1988;81: 1240–1246.
24. Yamaguchi T, Wakabayashi Y, Tanaka M, Sano T, Ishikawa H, Nakajima H, Suematsu M, et al. Taurocholate induces directional excretion of bilirubin into bile in perfused rat liver. Am J Physiol 1996;270:G1028–G1032.
25. Izumi Y, Yamazaki M, Shimizu S, Shimizu K, Yamaguchi T, Nakajima H. Anti-bilirubin monoclonal antibody. II. Enzyme-linked immunosorbent assay for bilirubin fractions by combination of two monoclonal antibodies. Biochim Biophys Acta 1988;967:261–266.
26. Mor-Cohen R, Zivelin A, Rosenberg N, Shani M, Muallem S, Seligsohn U. Identification and functional analysis of two novel mutations in the multidrug resistance protein 2 gene in Israeli patients with Dubin-Johnson syndrome. J Biol Chem 2001;276:36923–36930.
27. van der Kolk DM, de Vries EG, Noordhoek L, van den Berg E, van der Pol MA, Muller M, Vellenga E. Activity and expression of the multidrug resistance proteins P-glycoprotein, MRP1, MRP2, MRP3 and MRP5 in de novo and relapsed acute myeloid leukemia. Leukemia 2001;15:1544–1553.
28. Courtois A, Payen L, Lagadic D, Guillouzo A, Fardel O. Evidence for a multidrug resistance-associated protein 1 (MRP1)-related transport system in cultured rat liver biliary epithelial cells. Life Sci 1999;64:763–774.
29. Suematsu M, Suzuki H, Ishii H, Kato S, Yanagisawa T, Asako H, Suzuki M, et al. Early midzonal oxidative stress preceding cell death in hypoperfused rat liver. Gastroenterology 1992;103:994–1001.
30. Kajimura M, Shimoyama M, Tsuyama S, Suzuki T, Kozaki S, Takenaka S, Tsubota K, et al. Visualization of gaseous monoxide reception by soluble guanylate cyclase in the rat retina. FASEB J 2003;17:506–508.
31. Hayashi S, Takamiya R, Yamaguchi T, Matsumoto K, Tojo SJ, Tamatani T, Kitajima M, et al. Induction of heme oxygenase-1 suppresses venular leukocyte adhesion elicited by oxidative stress: role of bilirubin generated by the enzyme. Circ Res 1999;85:663–671.
32. Mottino AD, Cao J, Veggi LM, Crocenzi F, Roma MG, Vore M. Altered localization and activity of canalicular Mrp2 in estradiol-17beta-D-glucuronide-induced cholestasis. HEPATOLOGY 2002;35:1409–1419.
33. Kubitz R, D'Urso D, Keppler D, Haussinger D. Osmodependent dynamic localization of the multidrug resistance protein 2 in the rat hepatocyte canalicular membrane. Gastroenterology 1997;113:1438–1442.
34. Uchida K, Kanematsu M, Sakai K, Matsuda T, Hattori N, Mizuno Y, Suzuki D, et al. Protein-bound acrolein: potential markers for oxidative stress. Proc Natl Acad Sci U S A 1998;95:4882–4887.
35. Tanaka N, Tajima S, Ishibashi A, Uchida K, Shigematsu T. Immunohistochemical detection of lipid peroxidation products, protein-bound acrolein and 4-hydroxynonenal protein adducts, in actinic elastosis of photodamaged skin. Arch Dermatol Res 2001;293:363–367.

36. Ogawa K, Suzuki H, Hirohashi T, Ishikawa T, Meier PJ, Hirose K, Akizawa T, et al. Characterization of inducible nature of MRP3 in rat liver. Am J Physiol Gastrointest Liver Physiol 2000;278:G438–G446.
37. Gyenes M, De Groot H. Prostanoid release by Kupffer cells upon hypoxia-reoxygenation: role of pHi and $Ca^{2+}$. Am J Physiol 1993;264:G535–G540.
38. Johnston DE, Peterson MB, Mion F, Berninger RW, Jefferson DM. Synthesis and degradation of eicosanoids in primary rat hepatocyte cultures. Prostaglandins Leukot Essent Fatty Acids 1991;43:119–132.
39. Nakamura J, Nishida T, Hayashi K, Kawada N, Ueshima S, Sugiyama Y, Ito T, et al. Kupffer cell-mediated down regulation of rat hepatic CMOAT/MRP2 gene expression. Biochem Biophys Res Commun 1999; 255:143–149.
40. Roelofsen H, Soroka CJ, Keppler D, Boyer JL. Cyclic AMP stimulates sorting of the canalicular organic anion transporter (Mrp2/cMoat) to the apical domain in hepatocyte couplets. J Cell Sci 1998;111:1137–1145.
41. Kipp H, Arias IM. Intracellular trafficking and regulation of canalicular ATP-binding cassette transporters. Semin Liver Dis 2000;20:339–351.
42. Horton AA,Wood JM. Prevention of thromboxane B2-induced hepatocyte plasma membrane bleb formation by certain prostaglandins and a proteinase inhibitor. Biochim Biophys Acta 1990;1022:319–324
43. Kato Y, Shimazu M, Kondo M, Uchida K, Kumamoto Y, Wakabayashi G, Kitajima M, et al. Bilirubin rinse: a simple protectant against the rat liver graft injury mimicking heme oxygenase-1 preconditioning. HEPATOLOGY 2003;38:364–373.

# 代用血漿剤と臨床

Plasma Substitutes and Their Clinical Use

編著
川崎医科大学名誉教授 高折 益彦
昭和大学藤が丘病院 麻酔科助教授 小堀 正雄

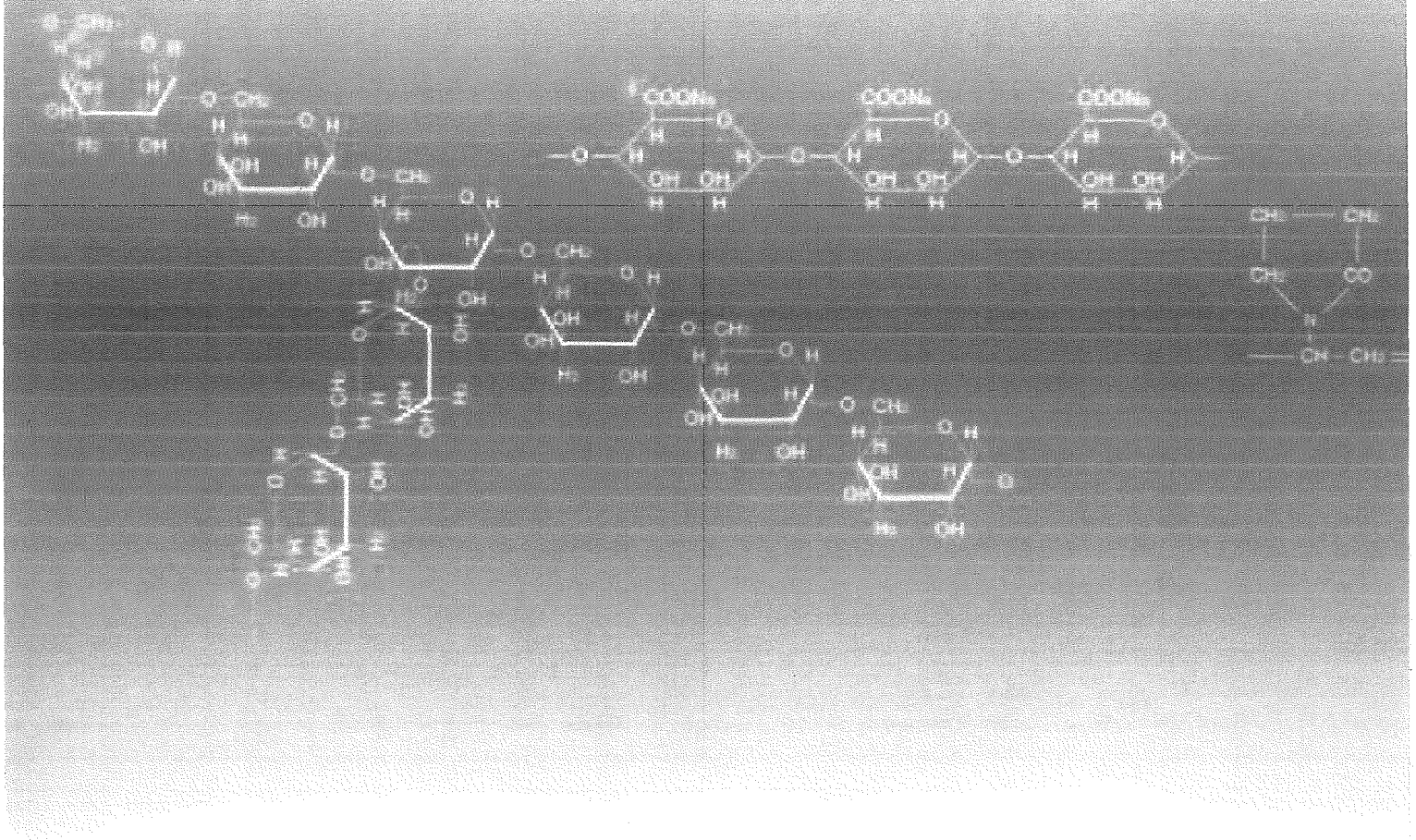

克誠堂出版

# 目　次

## 代用血漿剤　高折　益彦／1